Sea surface temperature signatures of oceanic internal waves in low winds

J. Tom Farrar
MIT-WHOI Joint Program in Physical Oceanography

Christopher Zappa
Lamont-Doherty Earth Observatory, Columbia University

Robert Weller
Woods Hole Oceanographic Institution

Andrew T. Jessup
University of Washington, Applied Physics Laboratory

March 5, 2006

Abstract

In aerial surveys conducted during the Tropical Ocean–Global Atmosphere (TOGA) Coupled Ocean–Atmosphere Response Experiment (COARE) and the low wind component of the Coupled Boundary Layer Air-Sea Transfer (CBLAST-Low) oceanographic field programs, sea surface temperature (SST) variability at relatively short spatial scales (10's of meters to kilometers) has been observed to increase under low wind conditions.

A unique data set of coincident surface and subsurface oceanic temperature measurements is used to investigate the subsurface expression of this spatially organized sea surface temperature variability, and it is shown that the SST signal is associated with oceanic internal waves. The data are used to test the two previously hypothesized mechanisms for SST signatures of oceanic internal waves: that internal wave signals in SST are caused by modulation of the cool-skin effect and that signals are caused by modulation of vertical mixing within the diurnal warm-layer. Under conditions of weak winds and strong insolation (which favor formation of a diurnal warm-layer), the data reveal a strong link between the spatially periodic SST fluctuations and subsurface temperature and velocity fluctuations associated with oceanic internal waves, suggesting that some mechanism involving the diurnal warm-layer is responsible for the observed internal wave signal. The lack of a clear internal wave signal in SST when no warm layer is present further suggests that the cool-skin straining may not be as effective a mechanism for producing internal wave signals in SST.

1 Introduction

Infrared (IR) imagery of the sea surface reveals a rich variety of patterns and coherent features at scales ranging from the cm scales of "microbreaking" waves to basin scales. Although many investigations have focused on either the smaller scales associated with surface wave processes (e.g. Jessup and Hesany, 1996; Jessup et al., 1997a, 1997b; Zappa et al., 2001, 2004; Jessup and Phadnis, 2005) or larger scales associated with meso- and basin-scale dynamics (e.g. Stumpf and Legeckis, 1977; Apel, 1980; Farrar and Weller, in press), a handful of recent papers have reported internal wave signals in infrared observations (Walsh et al., 1998; Marmorino et al., 2004; Zappa

and Jessup, 2005). Yet, adiabatic internal wave theory suggests that there should be no internal wave signal in sea surface temperature (SST), since a fluid element initially at the surface remains there for all time. More than one mechanism has been put forward to explain the existence of propagating SST signals associated with internal waves. Aside from the potentially important effects of this SST modulation on air-sea exchange and the atmospheric boundary layer, it is of interest to better understand these effects for remote sensing applications, particularly at low wind speeds when the surface roughness signal used to detect internal waves in synthetic aperture radar and other remote observations may be attenuated or absent.

This paper uses data collected during the low-wind component of the Coupled Boundary Layer Air-Sea Transfer experiment (CBLAST-Low; Edson et al., submitted manuscript) to examine the surface infrared signatures of oceanic internal waves and the mechanisms for these signatures. In addition to measurements of air-sea fluxes of heat, momentum, and moisture, this paper makes use of a unique data set consisting of collocated high-resolution airborne infrared imagery, shipboard infrared measurement, towed thermistor-chain measurements, and moored measurements of temperature and velocity.

Osborne (1965) predicted that internal waves (as well as surface waves) should have a signal in SST, based on the theory that vertical straining of the sea surface modifies the magnitude of the cool-skin effect. (The cool skin is an $O(1$ mm) thick conductive boundary layer that is cooler than the bulk fluid below because of latent, sensible, and long wave heat loss from the sea surface; the cool skin is in some ways analogous to the skin that forms on a warm bowl of stew or clam chowder.) Osborne's (1965) theoretical work is remarkable in part because the theory preceded, but is consistent with, the canonical theory of the cool skin later offered by Saunders (1967).

Walsh et al. (1998) observed quasi-periodic, propagating variations in IR SST measurements and argued compellingly that the variations were associated with oceanic internal waves. They proposed that the internal waves modulate vertical mixing within the strongly stratified layer that forms in the upper few meters during conditions of strong insolation and low winds. This interpretation was supported by the fact that nearby mooring data showed that internal waves caused temperature fluctuations as shallow as 0.5 m depth, but there were no coincident surface and subsurface measurements to unambiguously confirm the proposed mechanism.

Marmorino et al. (2004) observed quasi-periodic, propagating variations in IR imagery and convincingly interpreted these as being associated with internal waves. Marmorino et al. (2004) invoked a variation of Osborne's (1965) theory to account for the signal, but there were no subsurface data to corroborate this interpretation. Zappa and Jessup (2005) also observed spatially periodic structure in IR imagery and used nearby mooring data to argue that the signal was due to (nonlinear) internal waves; Zappa and Jessup (2005) appealed to the cool-skin straining mechanism (Osborne, 1965; Marmorino et al., 2004) as a likely explanation for the signal.

The observations of Walsh et al. (1998) and Marmorino et al. (2004) were collected in similar weather conditions. Both aerial surveys were carried out during the afternoon (1300-1800 local time) with wind speeds below 3 m/s. The observations of Zappa and Jessup (2005) were also collected in low winds, but their survey was conducted in the morning, around 0700 (local time). The observations examined in this study were also collected in low winds.

It remains an open question wether internal wave signals in SST are a low-wind phenomenon, but Hagan et al. (1997) and Walsh et al. (1998) noted that internal-wave scale patterns were observed in SST under low-wind conditions during the Tropical Ocean-Global Atmosphere (TOGA) Coupled Ocean-Atmosphere Response Experiment (COARE). We have qualitatively observed an increase of internal-wave scale SST variability during the CBLAST-Low experiment. For example, Figure 1 shows SST variance in the 100-1000 m wavelength band versus mean wind speed for 23 aerial SST surveys carried out during CBLAST-Low. A tendency for increased SST

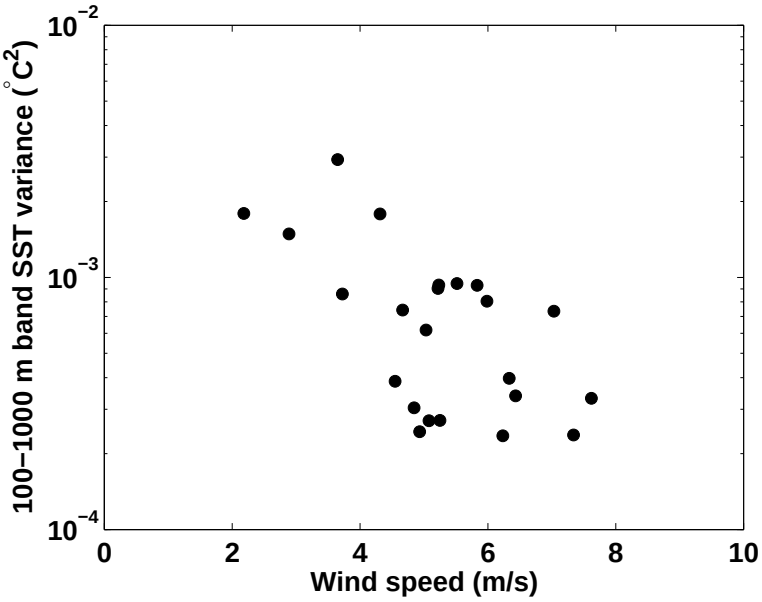

Figure 1: Surface temperature variance at 100-1000 m along-track scales from airborne infrared observations collected during the CBLAST-Low experiment (Section 3) versus mean wind speed during each flight.

variance at internal-wave scales during low winds is apparent, but we note that the relationship between wind speed and SST variance depicted in Figure 1 may be affected by the fact that different missions were carried out by the aircraft during the course of the experiment. In particular, sampling patterns were designed for each mission in part based on wind speed and SST variability.

An example of the 100-1000 m scale SST variability seen in low winds during the CBLAST-Low experiment is shown in Figure 2. These data were collected on August 15, 2003, the day corresponding to the point of largest 100-1000 m scale SST variance in Figure 1. The particular image shown in Figure 2 was selected because one of the surface moorings used in this study is visible in the image, but the SST signal is typical of what is observed and is similar to the signals seen in data presented by Marmorino et al. (2004) and Zappa and Jessup (2005).

This paper is organized as follows. Section 2 gives some details of the previously hypothesized mechanisms for the existence of internal-wave signals in SST and discusses our approach to testing these hypotheses using field data. Section 3 describes the data set and experimental design. In Section 4, the data are analyzed to demonstrate the connection between internal waves and examine the subsurface expression of the SST signal. Section 5 summarizes the results and discusses the implications of the observations for the hypothesized mechanisms.

2 Theory

The conditions considered by Walsh et al. (1998) and Marmorino et al. (2004) were similar to those during the afternoon survey described here (Section 3). All three sets of infrared skin-temperature measurements were collected during the afternoon (1300-1800 local time) under conditions of light winds (< 3 m/s), and all three data sets suggest the presence of spatially organized SST fluctuations associated with internal waves. Although these similarities suggest that the same mechanism may be responsible for the internal wave signal observed in SST, Walsh et al. (1998) and Marmorino et al. (2004) proposed different hypotheses for the existence of the signal. Marmorino et al. (2004) suggested that the internal wave signal resulted from modulation

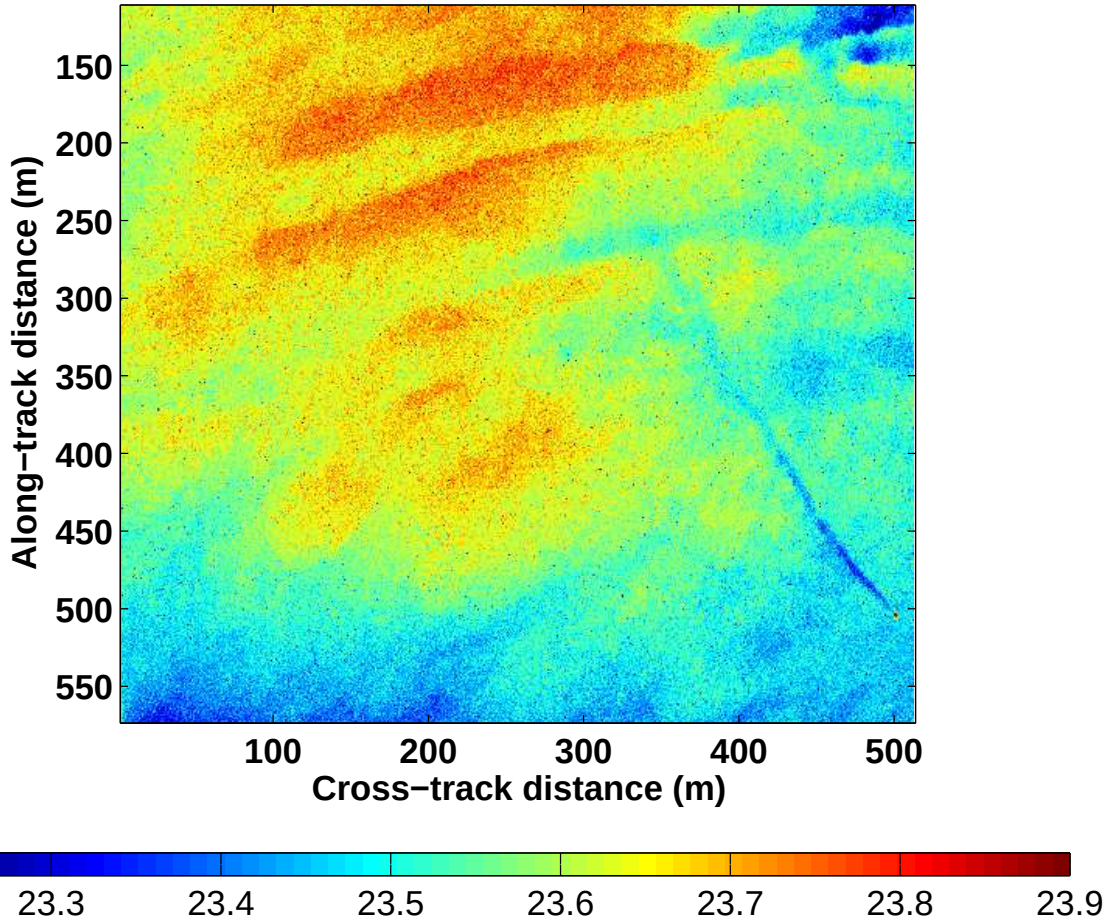

Figure 2: SST (°C). This is an example of quasi-periodic SST variability that is likely associated with internal waves. The data come from the airborne infrared measurements described in Section 3. The plane's heading was nearly due-north. One of the IMET buoys is visible in the lower-left corner as a warm circle with a long, cool wake trailing to the northwest. The buoy is warmer than the surrounding water because of radiant heating in the afternoon sun and low winds, and the wake is cool because the $O(1\text{ m})$ thick stratified warm-layer has been disrupted by the flow past the buoy.

of the O(1 mm) thickness of the cool skin, while Walsh et al. (1998) hypothesized that the SST signal resulted from modulation of the entrainment rate at the base of the diurnal warm layer (of O(1 m) thickness). An illuminating discussion of both the cool-skin and warm-layer effects is given by Fairall et al. (1996a). A primary goal of this study is to evaluate these two hypotheses using the extensive observations of skin temperature and subsurface temperature and velocity collected during the CBLAST-Low field campaign. Here, we give more detail about the type of surface signal expected under these two hypotheses.

2.1 Cool skin straining

Marmorino et al. (2004) hypothesized that the internal wave signal observed in IR SST measurements was due to cool-skin straining, based in part on the theoretical work of Osborne (1965), who offered a comprehensive study of the SST signal expected in a wide range of strain conditions, covering order-of-magnitude variations in amplitude and frequency of strain rate fluctuations. We will first summarize the effect of internal wave straining on the cool skin predicted by Marmorino et al. (2004) before reviewing Osborne's (1965) theory.

To estimate the effect of a fluctuating surface strain rate on the ocean-skin temperature, Marmorino et al. (2004) employed a linearized version of a model equation for the steady-state behavior of the cool skin in the presence of a positive surface strain (Equation 4.6 of Leighton et al. (2003)), noting that this equation is similar to Equation 19 of Osborne (1965). The equation used by Marmorino et al. (2004) is:

$$\Delta T = \sqrt{\frac{\pi}{2\kappa\alpha}}\left(\frac{Q}{\rho c_p}\right) \tag{1}$$

where α is the horizontal surface divergence (i.e. vertical strain rate), κ is the molecular diffusivity of heat, Q is the interfacial heat flux, ρ is the water density, and c_p is the specific heat. The approach of Marmorino et al. (2004) for predicting the skin temperature response to variations in the strain rate from internal waves was to use estimates of ΔT and Q from observations to estimate the ambient strain rate from Equation 1, finding $\alpha \approx 0.05$ s^{-1}. Then, Equation 1 was linearized about this value. Using the linearized equation,

$$T' = \alpha_{IW}\frac{\partial \Delta T}{\partial \alpha} \tag{2}$$

Marmorino et al. (2004) suggested that an oscillatory strain field of amplitude $\alpha_{IW} = 0.01$ s^{-1} would be sufficient to produce the observed SST variations. Marmorino et al. (2004) asserted that $\alpha_{IW} = 0.01$ s^{-1} is a reasonable value for the internal wave strain amplitude at the surface, but there were no concurrent *in situ* observations to support this claim. We note here that this strain rate implies a vertical velocity on the order of 1 cm/s at a depth of 1 m.

We find the kernel of the hypothesis of Marmorino et al. (2004) to be plausible, but their approach is likely to be quantitatively inaccurate. As one might guess from the infinitely-cold skin that Equation 1 gives for zero strain, this model solution is not appropriate for small strain values. Osborne (1965) states this explicitly in his discussion of his Equation 19; the solution is appropriate for values of α that satisfy $\alpha \gg \frac{\kappa}{\delta^2} \approx 0.1$ s^{-1}, where the approximate equality is obtained using $\kappa \approx 10^{-7}$ m^2/s and $\delta \approx 1$ mm. Thus, the ambient strain rate that Marmorino et al. (2004) inferred using Equation 1 is potentially outside of the range for which the equation is applicable, so the estimated sensitivity is possibly too large. Marmorino et al. (2004) claimed that the extreme sensitivity of Equation 1 to strain-rate variations at low strain values, coupled with low ambient strain values, is the reason that an internal wave signal is detectable in the the skin temperature. We find this claim dubious because inspection of Equation 1 suggests impossibly large (i.e., infinite) skin temperature signals when there is no background strain field.

It is possible to derive an expression similar to Equation 1 that is valid for all values of the strain rate (Osborne, 1965), but a precise theoretical expression for the cool-skin response to surface straining is not required to evaluate this hypothesis for the existence of an internal wave signal in SST under low-wind conditions.

2.2 Modulation of warm-layer entrainment

All three data sets were collected during conditions of light winds and strong insolation. During such conditions, heat and momentum are concentrated near the surface in a "diurnal warm layer" (Price et al., 1986; Fairall et al, 1996) that can exhibit temperature gradients as large as 4°C/m (e.g. Walsh et al., 1998 and references therein). The evolution of the warm layer can be modelled with surprising accuracy by assuming the depth of the layer is governed by a bulk Richardson number that remains on the threshold of criticality; the depth of the layer is then proportional to $I_\tau/\sqrt{I_Q}$ where I_τ and I_Q are the accumulated momentum and heat fluxes applied to the layer (Fairall et al., 1996).

Walsh et al. (1998) observed propagating patterns in infrared skin-temperature measurements from the western Pacific warm pool and made a convincing case that the patterns were associated with oceanic internal waves with periods of 30 min to 2 h. Walsh et al. (1998) examined temperature profiles from a nearby buoy and showed that internal waves modulated the depth of the O(1 m) thick warm layer by O(1 m). In light of this additional observation, Walsh et al. (1998) hypothesized that the observed SST signal was caused by modulation of entrainment at the base of the warm layer.

Within the context of the warm-layer model of Fairall et al. (1996), it stands to reason that modulation of the depth of the warm layer by internal waves should affect the entrainment at the base of the layer. The model requires that the Richardson number remain at the threshold of criticality, i.e.,

$$\frac{D\Delta T}{(\Delta U)^2} = C \tag{3}$$

where C is a constant (involving the critical Richardson number and physical constants) and ΔT and ΔU are the temperature and velocity differences between the base of the warm layer (depth D) and the surface. Though the Fairall et al. (1996a) warm-layer model does not explicitly consider advection, conservation of heat and momentum in the presence of vertical advection require that ΔT and ΔU are not directly affected by vertical advection. That is, vertical advection does not directly modify the surface properties or the temperature or velocity at base of the warm layer; it merely modifies the depth D over which the temperature and momentum gradients occur. Thus, an upward displacement of the base of the warm layer will initially reduce D, reducing the Richardson number below its critical threshold and causing an adjustment of ΔT, ΔU, and D to ensure that (3) is satisfied.

The near-surface mixing signal is irreversible; it is easy to imagine how the part of the wave with upward advection could produce a cool signal, but it is more difficult to imagine how downward advection of the base of the warm layer could produce a warm signal. (Marmorino et al. used an argument like this as evidence that the Walsh et al. hypothesis could not explain their observations.) Walsh et al. (1998) acknowledge this potential difficulty with their hypothesis and point out that one might expect the spatial pattern produced by such a mechanism to vanish after one complete wave cycle. They suggested that a more complex, nonrepeating internal wave field might always have a surface signal. However, it is conceivable that modulation of entrainment at the base of the warm layer, in conjunction with the positive heat fluxes required for the existence of a warm layer, could produce a warm anomaly of similar magnitude to what is observed. If we suppose that entrainment is shut off during the half-cycle that the vertical

velocity is downward, the change of temperature expected during that period would be

$$\Delta T' = \frac{Q\Delta t}{2\rho c_p D} \tag{4}$$

where Δt is the wave period. If the net heat flux applied to the layer (i.e., Q) has the modest value of 300 W/m^2, the wave period is 1 h, and D =O(1 m), the surface temperature would be expected to warm by 0.13°C. This warming is of the order of (or larger than) the warm anomalies observed by both Walsh et al. (1998) and Marmorino et al. (2004).

2.3 How can we test these hypotheses using field data?

The principal data set used in this paper consists of infrared measurements of SST (or, skin temperature) and coincident subsurface temperature measurements nominally spanning depths of 20 cm to 20 m (Section 3). We seek to determine whether the cool-skin straining hypothesis advocated by Marmorino et al. (2004) or the modulation of warm-layer entrainment hypothesis proposed by Walsh et al. (1998) provides a more plausible account for the prominent internal wave SST signal observed under low winds in CBLAST-Low.

The mechanism proposed by Marmorino et al. (2004) is purely a cool-skin effect. If a mechanism similar to the one proposed by Marmorino et al. (2004) is responsible for the internal wave signal observed in airborne infrared measurements of the skin temperature, we would expect the spatial pattern of the surface temperature signal to be quite similar to the spatial pattern of bulk-skin temperature difference, since the signal is hypothesized to result from variations in the bulk-skin temperature difference. Similarly, if the signal observed in the skin temperature is identical, or very similar, to the signal observed in the bulk fluid (20-30 cm depth), this would indicate that the SST signal results from processes in the bulk fluid and would thus constitute grounds for rejection of the Marmorino et al. hypothesis. In addition, the signal would be expected to be present regardless of the presence of a diurnal warm layer.

The mechanism proposed by Walsh et al. (1998) is not a cool-skin effect. If a mechanism similar to the one hypothesized by Walsh et al. (1998) is responsible for the internal wave signal, we would expect spatial or temporal fluctuations in the bulk water temperature (say, at 20 cm depth) to be nearly identical, in both amplitude and phase, to those measured at the surface. By the same logic, we would expect fluctuations in the bulk-skin temperature difference to have no systematic relationship to the fluctuations observed in the skin temperature.

Of course, it is conceivable that both mechanisms contribute to the observed variability. We will consider this possibility by analyzing data during times when no warm layer is present.

3 Data

The data were collected during the August 2003 Intense Observing Period of the CBLAST-Low field program, which took place in the coastal region south of Martha's Vineyard, Massachusetts. Some key observational elements of the field program were an oceanic mesoscale array of 14 moorings (Figure 3), the Air-Sea Interaction Tower (ASIT; Edson et al., submitted manuscript), aircraft surveys, and ship surveys. The field program took place in water depths ranging from 10-50 m. The area is characterized by light to moderate winds, the passage of synoptic weather systems, and a strong thermocline during the summer.

Three moorings within the oceanic mesoscale array were instrumented heavily with subsurface vertical temperature/salinity arrays as well as velocity measurements. In situ measurements of precipitation, relative humidity, wind speed and direction, incoming short and long wave radiation, and air temperature were also made at these three fixed locations (Colbo and Weller,

submitted manuscript; Edson et al., submitted manuscript). These surface meteorological measurements were used with the TOGA-COARE bulk flux algorithm (Fairall et al., 1996b, 2003) to estimate the air-sea fluxes of heat, momentum, and moisture. In addition, there were 11 other moorings measuring temperature in the region (Figure 3). These measurements allow a detailed description of the spatial and temporal evolution of surface meteorology and subsurface density and velocity within the approximately 20 by 30 km study region.

Shipboard operations were conducted from the *FV Nobska*. A bow-mast on the *Nobska* was equipped with upward and downward looking Heitronics model KT-19.82 infrared radiometers (8-14 μm) to accurately measure the ocean skin temperature (corrected for sky reflection) at a 1 Hz sampling frequency. The KT-19 was calibrated in the laboratory, but due to a temperature dependence in the response of the instrument, the resulting SST showed a warm bias. We estimated the magnitude of this bias by comparing the shallowest subsurface temperature measurement ($\sim$30 cm) to the SST during nighttime conditions when a net heat loss from the ocean surface leads to a cool skin. This comparison suggested the estimated SST was at least 0.5°C too warm. The estimated bias is calculated at the time of minimum heat loss during the nighttime, when the cool skin effect is expected to be minimal. Any residual bias is well within the expected accuracy of the system in laboratory conditions, but it is worth noting that the conclusions of this paper are not affected by radiometer bias since the hypotheses are evaluated by comparison of fluctuations in the bulk and skin temperature.

The *Nobska* also carried a complete direct covariance flux package (Edson et al., 2004) and radiometers for measuring incident short and long wave radiation (Colbo and Weller, in press/submitted). Subsurface temperature/salinity measurements were made using 21 Seabird SBE 37's and SBE 39's sampled at 4 or 5 seconds. The instruments were towed from the *Nobska's* boom crane, and care was taken to ensure that the instrument chain was as far as possible to the side of the vessel's wake. The towed instrument chain could be deployed with vertical spacing greater than or equal to 0.5 m. The horizontal distance between oceanographic samples depends on the vessel's speed (5-7 kts) and the sampling rate (0.2-1 Hz); the nominal horizontal separation between SST measurements was 2 m and the separation between sequential subsurface measurements was about 8 m. Aliasing of surface waves is a concern, but for the low wind conditions under consideration here, the seas were calm and surface wave activity was minimal.

Three of the subsurface instruments measured pressure. The 10th and 12th instruments were SBE 39 temperature/pressure recorders and a RBR DR-1050 was at the bottom of the "chain". Prior to analysis, all records were linearly interpolated to a common 4-second time base and the pressure records were used to estimate the actual depth of each instrument through time as follows. Given the nominal depth that each sensor would assume if the chain hung vertically, the angle from the surface to each of these 3 pressure measurements was estimated as $\cos^{-1}$(measured depth/nominal depth). This gives 3 estimates of the angle. Typically, the three estimates agreed to within 20°, and the largest angles were found for the deepest sensor. These three estimates were averaged to obtain a single estimate for the angle of the chain with respect to the surface. (Although the chain is expected to take on something like catenary shape, the chain appeared to be straight in the upper few meters.) Finally, an offset (typically 0-0.5 m) was applied to ensure that the depth of sensor #10 (the shallowest pressure measurement) matched the value inferred from the observed pressure. The depth estimation method was "successful" in the sense that the estimated depth of the shallowest sensor agreed with visual estimates of the depth made from the deck of the *FV Nobska* during the surveys. The estimated depths are expected to be most accurate near the surface, where the angle of the line amounts to a small depth correction. This method of estimating the depth (mandated by the small number of pressure sensors) is obviously imperfect. However, inaccuracies in the estimated measurement depths do not affect the conclusions of this paper.

The airborne infrared measurements were made using the Univ. Washington Applied Physics

Laboratory's Infrared System (APLIS), which was developed during CBLAST-LOW to address two concerns. A primary concern regarding the use of an IR camera to measure sea surface temperature is the ability to acquire data during the day, when solar reflections are present. A second concern is the ability to discriminate between real skin temperature variations and apparent variations caused by reflections from clouds. APLIS consists of two sensor pairs that include a high-resolution, low-noise AIM model 640Q longwave (8-10 or 8-9.5 μm) IR camera (512 x 640 pixels) and a calibrated Heitronics model KT-15.82 narrow field-of-view radiometer (8-14 μm). One sensor pair is directed near-nadir to measure sea surface radiance and the other is directed upward to measure sky radiance. This combination of sensors provides high-resolution, low noise imagery of calibrated, sky-corrected sea surface temperature. The IR cameras used in the current system are based on a longwave QWIP array, which provides superior imagery. In addition to providing high resolution, the longwave cameras can be used during the day with minimal contamination due to reflected sunlight. Images were acquired at 1 Hz in order to provide an instantaneous 2-D map of surface temperature with a thermal resolution of roughly 0.02°C. For the nominal altitude of 875 m in 2003, the spatial resolution was less than 0.9 m. A down-looking Pulnix digital video camera was implemented to supplement the IR measurements and to characterize the sea surface condition. During the 2003 CBLAST-Low experiments, APLIS was deployed aboard a Cessna Skymaster aircraft operated by Ambroult Aviation (Chatham, MA).

We have identified a useful case study of enhanced SST variability in low winds utilizing ship, mooring, and aircraft data from Aug 15, 2003. Winds were low-to-moderate throughout the day, with wind speeds of 2.5-4.5 m/s in the early morning hours decreasing to speeds of 1-2 m/s by about noon local time. We carried out nearly overlapping ship transects (Figure 3), one around 7:30 and another around 16:30 (local time). During both surveys, coincident radiometric SST measurements and subsurface temperature and salinity measurements were collected. Both sections were about 10 km long in a cross-shore direction and spanned water depths of about 22-37 m. Each transect took about 70 min to complete. The mean wind speeds and surface turbulent heat fluxes were very similar during the two transects, but the low winds and strong daytime heating led to the development of very strong, shallow temperature stratification, with a temperature gradient of about 2°C over the upper 2 m. This strong temperature gradient and the thickness of this "warm layer" are roughly consistent with the scaling analysis of Price et al., 1986. During the afternoon survey, the Cessna Skymaster flew almost directly over the *FV Nobska* along a similar track (Figure 3). The shipboard infrared SST measurements indicated that the 100-2000 m SST variability was much larger during the afternoon survey. We have chosen to focus on this case study because it will allow a more direct evaluation of the Marmorino et al. (2004) and Walsh et al. (1998) hypotheses than has been possible with previous data sets. In addition, this directly addresses a central CBLAST-Low goal of understanding SST and boundary layer variability under low winds.

Unless otherwise specified, all times are local (i.e. Eastern Time, equal to UTC minus four hours), and all smoothing and bandpass filtering is carried out using a moving-average filter.

4 Results

4.1 Observed Subsurface Expression of Low Wind SST Variability from *F/V Nobska*

The evolution of wind speed, surface heat flux, and near surface thermal structure on August 15, 2003 are summarized in Figure 4 using data from a nearby buoy. The pairs of vertical black lines mark the times of the two survey sections that are discussed here. The wind speed was low-to-moderate throughout the day, only exceeding 3 m/s for several hours up to 07:30 (local) and after 18:00 (local). The moderate wind speeds of the early morning hours and nighttime

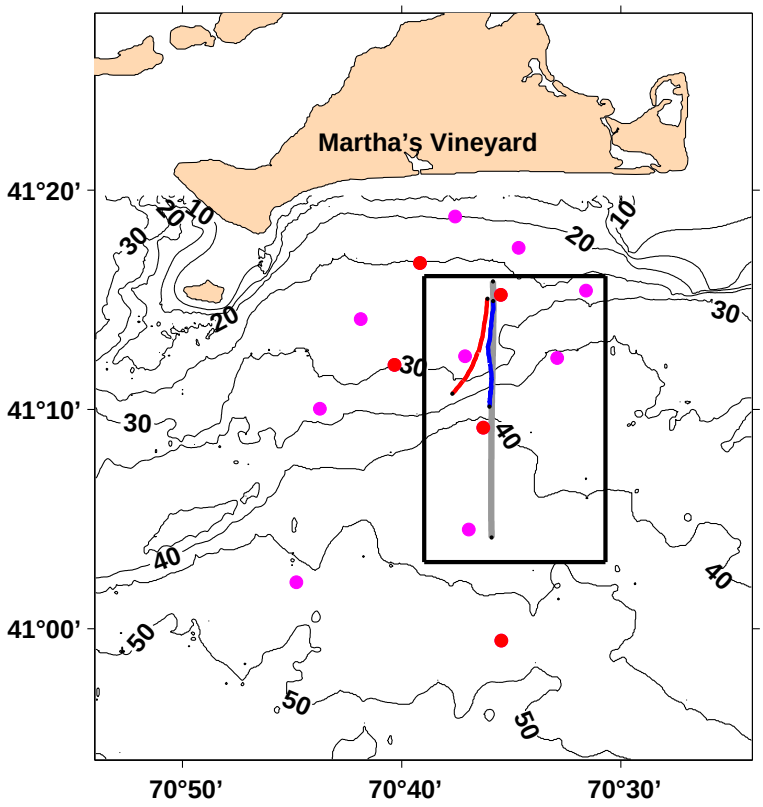

Figure 3: The morning survey section (blue line) and the late-afternoon section (red line) from August 15, 2003. The aircraft survey track is indicated by a gray line. Also shown are the mooring locations for the CBLAST-Low Intense Observing Period of August, 2003 (pink and red circles).

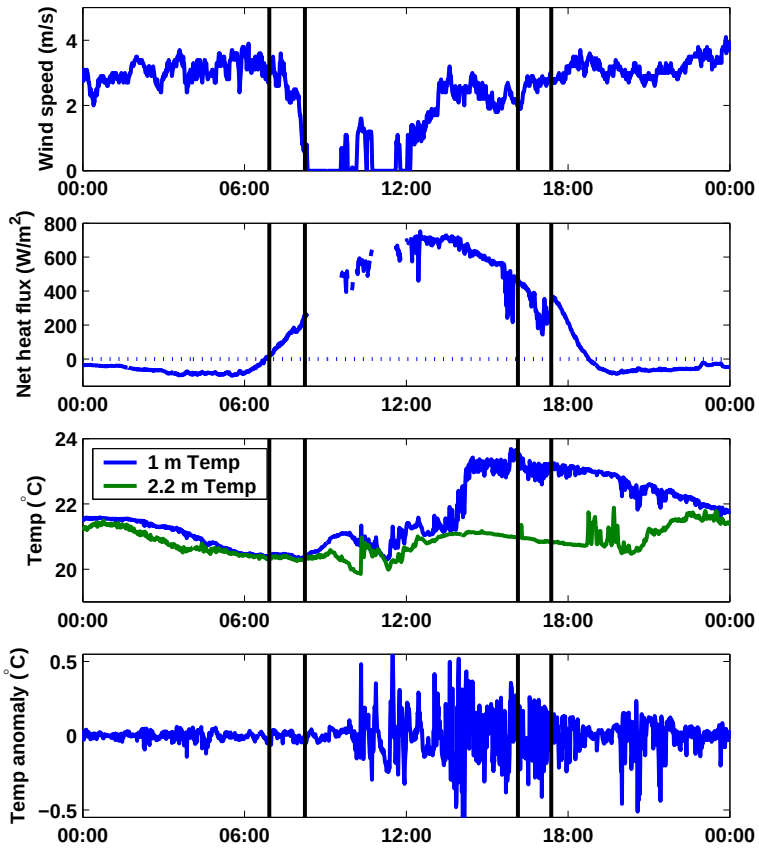

Figure 4: Data from a surface buoy near the termination point of the two transects. The time of each transect is marked by a pair of vertical black lines. Top panel: Wind speed. Second panel: Net heat flux into the ocean. Third panel: Subsuface temperature at the 1 m and 2.2 m levels (blue and green lines, respectively). Lower panel: Temperature anomaly at 1 m depth relative to a 1 hour running average.

cooling of the sea surface facilitated the formation of a fairly well-mixed surface layer as is indicated by the relatively small temperature difference between the 1 m and 2.2 m levels. Around 08:30 (local), the wind speed dropped below the detection threshold of the anemometer, and near surface thermal stratification increased rapidly. The lower panel of Figure 3 shows the temperature anomaly relative to a 1-hour running average. As the near surface stratification increased, so did the variability in 1 m temperature. The temperature difference between the 1 m and 2.2 m levels was about 2°C for much of the afternoon, so perhaps it should not be surprising that the temperature variability should be relatively large in the presence of such an extreme temperature gradient.

The rapid warming of the sea surface during the day is reflected in the difference of SST observed in the morning and afternoon surveys, which exceeded 2.5°C at most locations along the track. Figure 5 shows the observed SST along the two survey tracks and the corresponding temperature anomalies relative to a 1 km running average. The sub-kilometer scale variability in SST was significantly larger during the afternoon survey.

A cool skin is expected to have been present during both transects. Measurements from the buoys near the endpoints of the ship transects indicate that the surface heat fluxes were very similar during the morning and afternoon surveys. For example, the combined latent, sensible, and long wave heat loss from the sea surface at the buoy nearest the southern end of the two transects averaged 108 W/m^2 during the morning survey and 111 W/m^{2}during the afternoon survey. Although the average net solar radiation was about twice as large during the afternoon

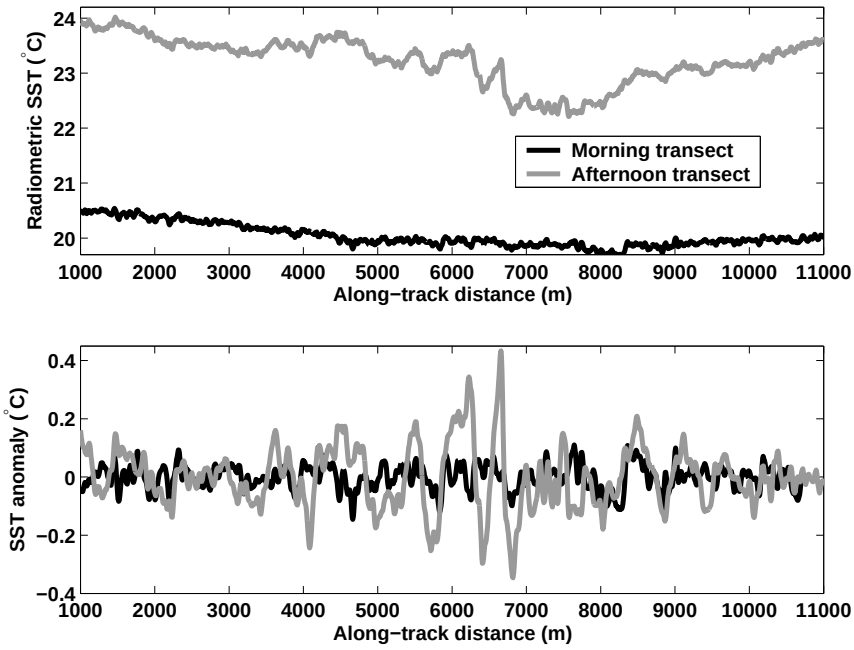

Figure 5: Upper panel: Radiometric SST observed along the morning and afternoon survey tracks. Lower panel: SST anomaly relative to a 1 km running average. The sub-kilometer scale spatial variability in SST was considerably larger during the afternoon transect.

survey (388 versus 203 W/m^2), the solar heating was not large enough to negate the cool-skin effect. Assuming that roughly 6.7% of the net solar radiation is absorbed within the skin layer (Wick et al., 2005), the average net surface heat loss from the skin layer was 94 W/m^2 during the morning survey and 85 W/m^2 during the afternoon survey. Thus, the magnitude of the cool skin effect is expected to have been comparable during the two surveys.

The near surface stratification was relatively weak during the morning survey, and the variability in near surface temperature was small (Figure 6, upper panel). A strong vertical temperature gradient of O(1°C m^{-1}) was present at 5-15 m depth, and this thermocline deepened and weakened toward the coast. Above this thermocline, surface and subsurface temperature fluctuations were modest during the morning survey. Quasi-periodic isothermal excursions were observed in the main thermocline along the entire track; these fluctuations are associated with vertical displacements of isotherms by the oceanic internal wave field.

The surface and subsurface thermal structure observed during the morning survey can be contrasted with that observed during the afternoon survey (Figure 6, lower panel). The thermal structure in and below the main thermocline remained relatively similar to that seen during the morning survey. However, over the course of the day, a substantial temperature gradient had developed just below the surface, having a value of about 1°C m^{-1} on the upper meter over most of the section. This very shallow thermocline, located in the upper 2 m of the water column, is comparable in strength to that of the main thermocline. As a consequence, there are substantial temperature anomalies extending near the surface in association with vertical advection by the internal wave field.

The along track temperature anomalies from the two surveys are shown in Figure 7. These temperature anomalies were computed by band-passing the along-track temperature data at 50-1000 m scales. During the morning survey, temperature anomalies were relatively small above the main thermocline (located at 5-15 m depth), typically less than 0.05°C. In contrast, the afternoon survey shows strong temperature anomalies in the upper few meters, coherent with fluctuations at greater depths.

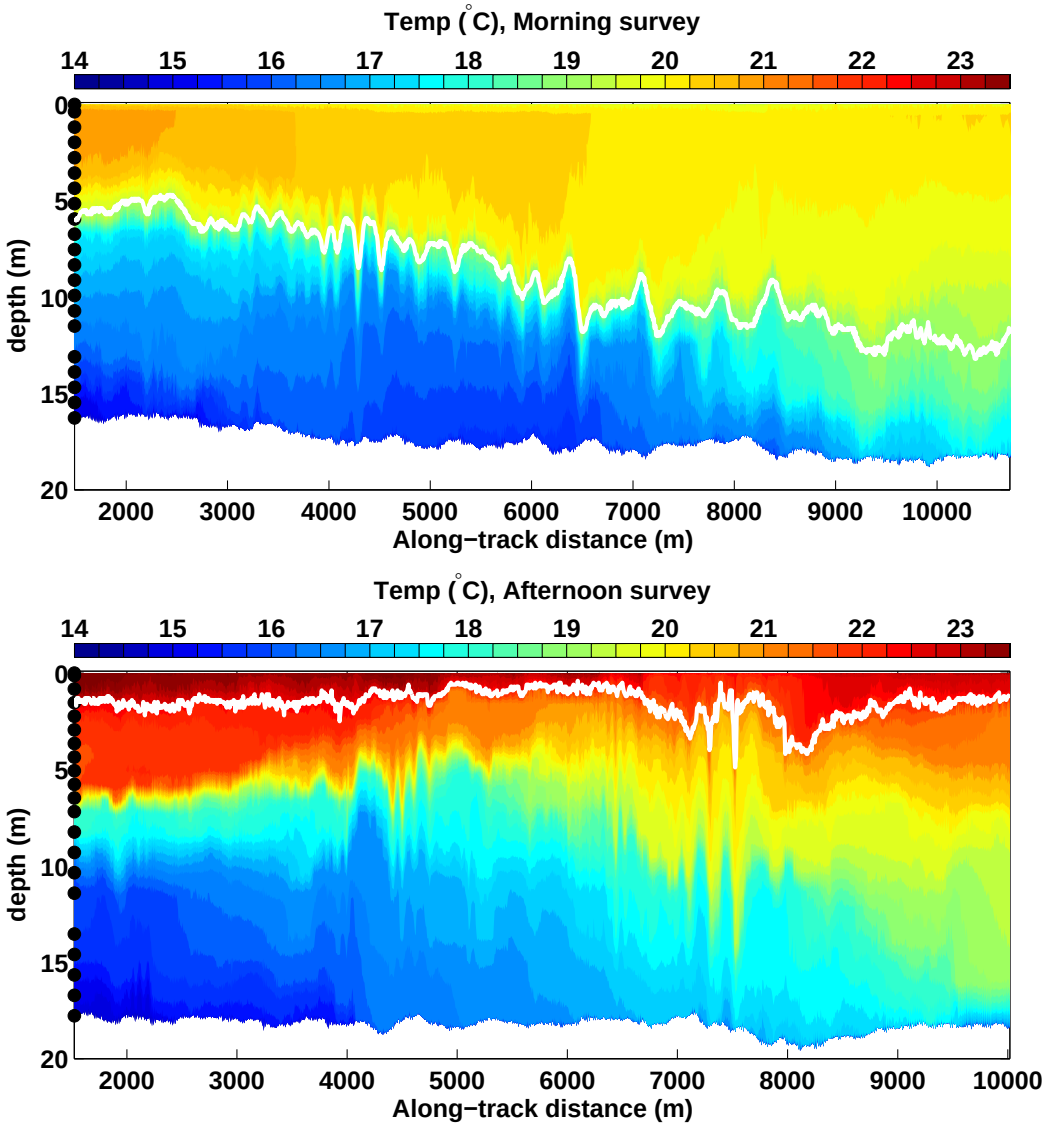

Figure 6: Temperature data from the morning survey section (upper panel) and afternoon section (lower panel). The black dots on the left side of each panel mark the nominal instrument depths, and the heavy white lines marks the depth where the temperature is 1°C less than the SST.

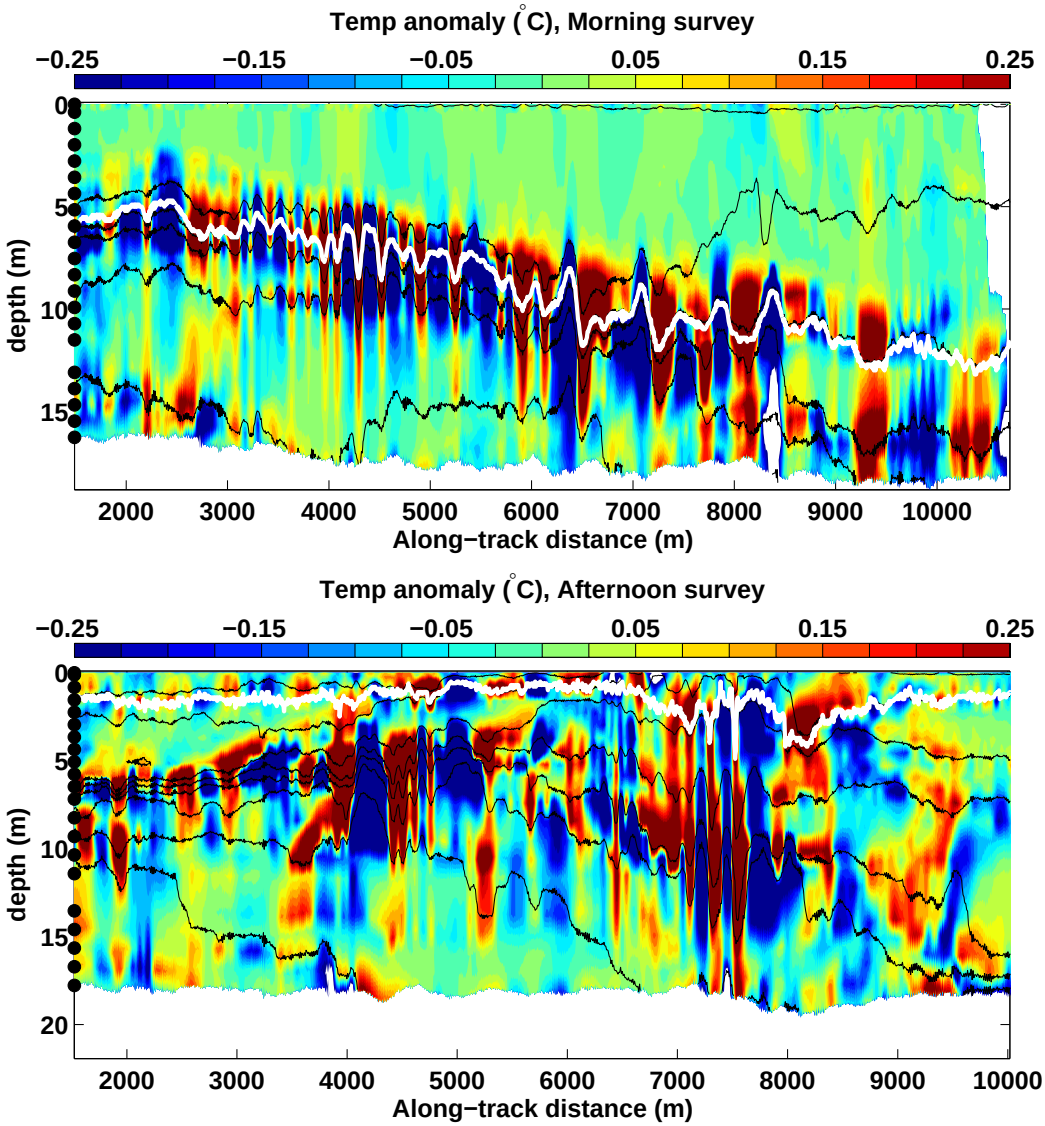

Figure 7: Temperature anomaly along the morning survey section (upper panel) and afternoon section (lower panel). The anomalies are computed by band-passing the temperature at 50-1000 m scales. The black dots on the left side of each panel mark the nominal instrument depths. The black lines mark isotherms at 1°C intervals, and the heavy white lines marks the depth where the temperature is 1°C less than the SST.

4.2 Internal wave signals as seen in aircraft and moored measurements under low-wind conditions

Aircraft surveys quantified the horizontal variability of SST in the CBLAST-Low study region. Real-time display of SST data on the Cessna and the *FV Nobska* indicated that the 10-2000 m SST variability was unusually large during the low-wind conditions of August 15. Ship and aircraft teams, communicating by radio, then devised a strategy to optimally utilize the ship, aircraft, and moorings to better characterize and understand this low-wind SST variability through overlapping surveys (Figure 3). (The *Nobska* changed course to align with the morning survey section and the aircraft's flight pattern, which is part of the explanation for the curvature of the *Nobska's* track during the afternoon survey.) While the drastic difference in the speed of the aircraft and the ship precludes direct comparison of the measurements made on the two platforms, the internal wave signal in the aircraft measurements can be compared with the internal wave characteristics inferred from the moored measurements of temperature and velocity.

Because of the speed of the aircraft and the infrared imagers aboard the aircraft, the aircraft observations of SST allow a better spatial description of the spatial variability of SST than is possible from the shipboard observations. Successive 444 m $\times$ 555 m images of SST can be patched together to form an along-track swath of 444 m width (Figure 8). In constructing this swath, we ignored the gradual deviations of the aircraft's flight track from a due-north straight line. (As can be seen in Figure 3, the aircraft flew in a nearly straight line, and the maximum deviation from the mean longitude did not exceed 90 m over the 20 km track.) We also ignored the subtle image distortion associated with the look-angle of the imager. The SST swath observed on the afternoon of Aug 15, 2003 reveals the presence of wavelike SST variations at a variety of scales. When inspecting the entire swath, the wavelike features that are most apparent have an along-track length scale on the order of 1 km with crests oriented toward the northeast. Features with scales of O(100 m) are also apparent, as can be seen in Figure 2, which shows a close-up on part of the image shown in Figure 8 from the vicinity of the mooring near the northern end of the swath.

Additional evidence that the wavelike signal observed in SST is in fact due to internal waves comes from analysis of data from the nearby moorings. The mooring data indicated the presence of quasi-linear, energetic internal waves with a period of about 30 minutes during the time of the aircraft overpass. For such high frequency internal waves, the earth's rotation can be neglected, so the horizontal velocity signal of the wave is expected to be rectilinear and normal to the wave crests (i.e. down the pressure gradient). The 20-60 minute band-passed velocity vectors are roughly rectilinear and normal to the crests and troughs seen in the SST imagery (Figure 9), suggesting that the 30 minute period internal waves may be responsible for the wavelike signal observed in SST. This evidence is less direct than the coincident surface-subsurface observations from the *FV Nobska*, but taken with the ship observations showing a close link between skin temperature fluctuations and subsurface temperature fluctuations due to internal waves, we believe it is a sound inference that the regular pattern of skin temperature variability seen in the aircraft IR imagery is associated with the internal waves observed at the moorings.

It would be desirable to obtain an independent estimate of the wavelength of the internal waves observed at the mooring site. If mean flow effects could be neglected and the internal wave dynamics were linear and hydrostatic, it would be possible, in principle, to accurately estimate the wavelength and propagation direction of the waves by examining the transfer function between velocity and dynamic height fluctuations. Assuming linear dynamics might be justifiable and waves longer than about 100 m should be essentially hydrostatic, but the strong tidal flow in the region is likely to cause substantial Doppler shifting of the internal waves. Lacking knowledge of the intrinsic frequency of the waves, an estimate of the wavelength from the mooring data by a spectral technique would likely have large errors. The relative error in a transfer function

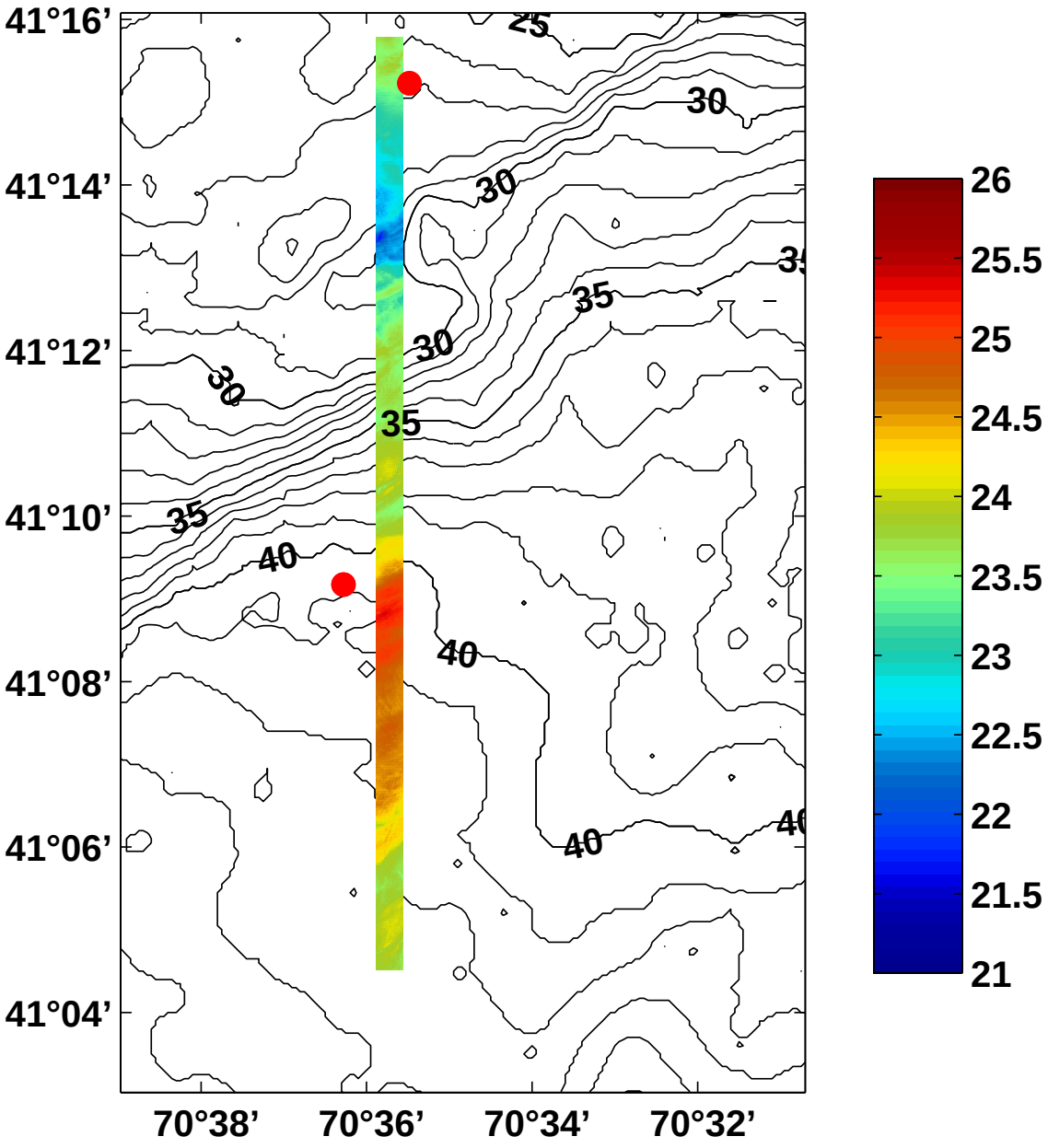

Figure 8: Airborne SST (°C). The axes correspond to the black box on Figure 3. The filled red circles mark the locations of air-sea interaction moorings.

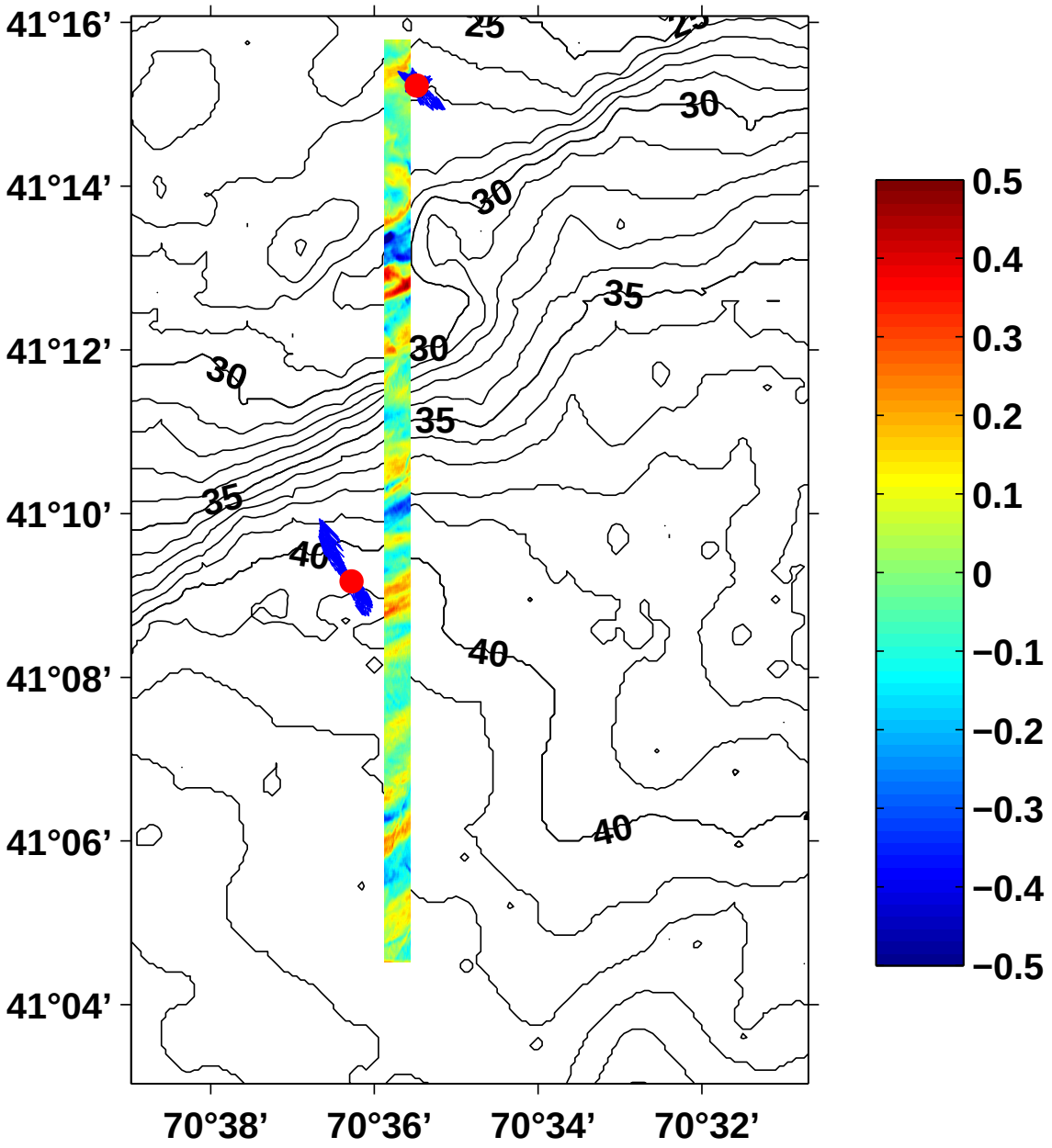

Figure 9: SST anomaly relative to 1.7 km along-track smoothed field. The filled red circles mark the positions of moored current meters, and the blue arrows are 20-60 minute band-passed velocity vectors at depths of 9 m (northern mooring) and 8 m (southern mooring). The velocity vectors are expected to be normal to the the internal wave crests, and they can be seen to be approximately normal to the “crests” in the SST anomaly.

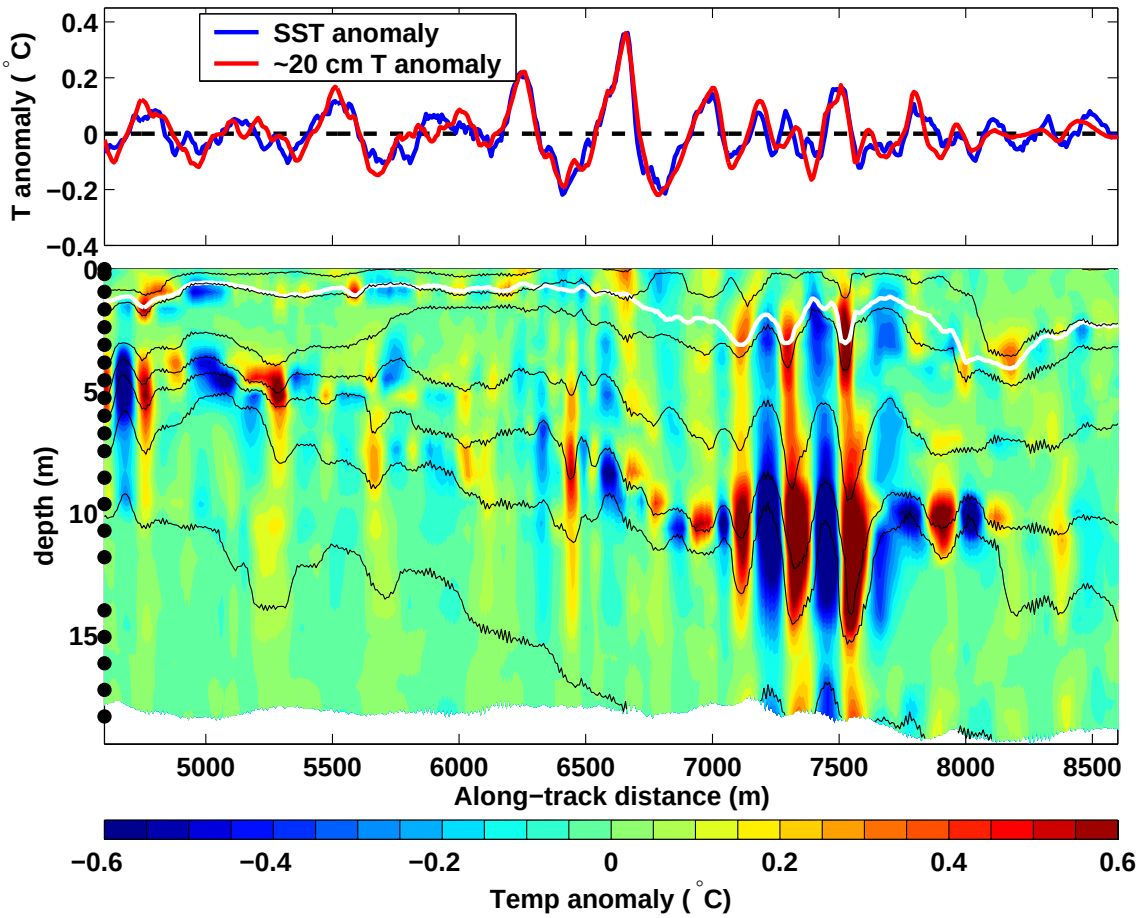

Figure 10: 50-300 m along-track band-passed temperature during the afternoon survey. Upper panel: Signal in SST and the shallowest subsurface temperature measurement (mean depth of 20 cm during the interval shown). Lower panel: Signal in subsurface temperature. The black dots on the left side of the figure mark the nominal measurement depths. The black lines mark isotherms at 1°C intervals, and the heavy white line marks the depth where the temperature is 1°C less than the SST.

estimate of the wave number vector is expected to be given by the ratio of the frequency Doppler shift to the observed frequency. A worst-case estimate (assuming the wave number is aligned with the mean flow) suggests that the error in such an estimate could exceed 60%. We did estimate the wave number by a transfer function approach and obtained wavelengths and orientations comparable to those seen in SST, but we will not report the details of those calculations here because of the large uncertainty in the estimate. The estimate of the propagation direction in the previous paragraph is insensitive to Doppler shifting by the mean flow.

5 Discussion and conclusion

The coincident surface-subsurface shipboard observations and the relationship between the airborne observations of spatially regular SST fluctuations and the internal wave signals in the mooring data suggest that the observed SST fluctuations are associated with oceanic internal gravity waves. The internal wave field found during the morning ship survey was similar to that seen in the afternoon survey (e.g., in the vertical displacement of the main thermocline), yet the SST signal was much larger in the afternoon survey.

The fact that the fluctuations in SST observed from the *FV Nobska* closely mimic those observed in the near-surface bulk temperature (Figure 10) strongly suggests that the organized SST fluctuations observed from both the ship and aircraft are not due to the cool-skin effect hypothesized by Osborne (1965) and Marmorino et al. (2004). To our knowledge, the data presented here are not inconsistent with the hypothesis of Walsh et al. (1998) that vertical advection by internal waves modulate vertical mixing within the strongly stratified warm layer that forms under conditions of strong insolation and low winds. Internal wave theory suggests that some diabatic process is required for internal waves to produce an SST signal, and the Walsh et al. (1998) mechanism is a plausible explanation for modulation of vertical mixing. Preliminary numerical experiments in which an internal wave vertical velocity signal is incorporated into the Price et al. (1986) mixed-layer model suggest that the warm-layer mechanism can produce surface temperature fluctuations similar to those observed.

Our failure to detect an internal wave signal in the bulk-skin temperature difference obviously does not imply that the cool-skin straining mechanism cannot produce an observable SST signal. However, it does suggest that cool-skin straining by internal waves is a less effective mechanism for producing a signal in SST. Zappa and Jessup's (2005) observations showed an internal wave SST signal at a time when there was no evidence of a diurnal warm layer, so the warm-layer hypothesis of Walsh et al. (1998) cannot explain that signal.

Of course, there could be other mechanisms that might modulate near surface mixing in the warm layer. For example, the vertical shear of the horizontal velocity of the waves and its orientation to the wind-driven shear may serve to modulate near-surface mixing, or the wind-driven velocity may even "shear the tops off of the internal waves" to cause convective instabilities. The fact that the early morning survey revealed no systematic relation between surface and subsurface temperature fluctuations implies that the large signals observed from the ship and aircraft in the afternoon depend in some way on the presence of the warm layer. We are presently working to better understand the mechanism by which the internal waves produce a signal in SST.

Acknowledgements

We gratefully acknowledge funding for this research through the CBLAST Departmental Research Initiative.

References

[1] J.R. Apel. Satellite sensing of ocean surface dynamics. *Ann. Rev. Earth Planet. Sci.*, 8:303–342, 1980.

[2] K. Colbo and R.A. Weller. The accuracy of the IMET sensor package. *Manuscript submitted to J. Atmos. Oceanic Technol.*, 2006.

[3] J.B. Edson and co authors. The Coupled Boundary Layers and Air-Sea Transfer experiment in low winds (CBLAST-LOW). *Bull. Am. Met. Soc.*, Submitted manuscript.

[4] J.B. Edson, C.J. Zappa, Ware J.A., W.R. McGillis, and J.E. Hare. Scalar flux profile relationships over the open ocean. *J. Geophys. Res.*, 109:doi:10.1029/2003JC001960, 2004.

[5] C.W. Fairall, E.F. Bradley, J.E. Hare, A.A. Grachev, and J.B. Edson. Bulk parameterization of air-sea fluxes: Updates and verification for the COARE algorithm. *J. Climate*, 16:571–591, 2003.

[6] C.W. Fairall, E.F. Bradley, D.P. Rogers, J.B. Edson, and G.S. Young. Bulk parameterization of air-sea fluxes during TOGA COARE. *J. Geophys. Res.*, 101:3747–3764, 1996.

[7] C.W. Fairall, J.S. Bradley, E.F. Godfrey, G.A. Wick, J.B. Edson, and G.S. Young. The cool skin and warm layer in bulk flux calculations. *J. Geophys. Res.*, 101:1295–1308, 1996.

[8] J.T. Farrar and R.A. Weller. Intraseasonal variability near 10°N in the eastern tropical Pacific Ocean. *J. Geophys. Res.*, in press.

[9] D.E. Hagan, D.P. Rodgers, C.A. Friehe, R.A. Weller, and E.J. Walsh. Aircraft observations of sea surface temperature variability in the tropical Pacific. *J. Geophys. Res.*, 102:15733–15747, 1997.

[10] A.T. Jessup and V. Hesany. Modulation of ocean skin temperature by swell waves. *J. Geophys. Res.*, 101:6501–6511, 1996.

[11] A.T. Jessup and K.R. Phadnis. Measurement of the geometric and kinematic properties of microscale breaking waves from infrared imagery using a piv algorithm. *Meas. Sci. Tech.*, 16:1961–1969, 2005.

[12] A.T. Jessup, C.J. Zappa, M.R. Loewen, and V. Hesany. Infrared remote sensing of breaking waves. *Nature*, 385:52–55, 1997a.

[13] A.T. Jessup, C.J. Zappa, and H. Yeh. Defining and quantifying microscale wave breaking with infrared imagery. *J. Geophys. Res.*, 102:23145–23153, 1997b.

[14] R.I. Leighton, G.B. Smith, and R.A. Handlerb. Direct numerical simulations of free convection beneath an airwater interface at low Rayleigh numbers. *Phys. Fluids*, 15:3181–3193, 1995.

[15] G.O. Marmorino, G.B. Smith, and G.J. Lindemann. Infrared imagery of ocean internal waves. *Geophys. Res. Lett.*, 31:doi:10.1029/2004GL020152, 2004.

[16] M.F.M. Osborne. The effect of convergent and divergent flow patterns on infrared and optical radiation from the sea. *Deutsche Hydrographische Zeitschrift*, 18:1–25, 1965.

[17] J.F. Price, R.A. Weller, and R. Pinkel. Diurnal cycling: observations and models of the upper ocean response to diurnal heating, cooling, and wind mixing. *J. Geophys. Res.*, 91:8411–8427, 1986.

[18] H.G. Stumpf and R.V. Legeckis. Satellite observations of mesoscale eddy dynamics in the eastern tropical Pacific Ocean. *J. Phys. Oceanogr.*, 7:648–658, 1977.

[19] E.J. Walsh, R. Pinkel, D.E. Hagan, R.A. Weller, C.W. Fairall, D.P. Rodgers, S.P. Burns, and M. Baumgartner. Coupling of internal waves on the main thermocline to the diurnal surface layer and sea surface temperature during the Tropical Ocean-Global Atmosphere Coupled Ocean-Atmosphere Response Experiment. *J. Geophys. Res.*, 103:12613–12628, 1998.

[20] G.A. Wick, J.C. Ohlmann, C.W. Fairall, and A.T. Jessup. Improved oceanic cool-skin corrections using a refined solar penetration model. *J. Phys. Oceanogr.*, 35:1986–1996, 2005.

[21] C. Zappa and A.T. Jessup. High resolution airborne infrared measurements of ocean skin temperature. *Geosciences and Remote Sensing Lett.*, 2:146–150, 2005.

[22] C.J. Zappa, W.E. Asher, and A.T. Jessup. Microscale wave breaking and air-water gas transfer. *J. Geophys. Res.*, 106:9385–9391, 2001.

[23] C.J. Zappa, W.E. Asher, A.T. Jessup, J. Klinke, and S.R. Long. Microbreaking and the enhancement of air-water transfer velocity. *J. Geophys. Res.*, 109:doi: 10.1029/2003JC001897, 2004.